

Article

Experimental Study on the Treatment of Landfill Leachate by Electro-Assisted ZVI/UV Synergistic Activated Persulfate System

Baojun Jiang ^{*}, Jianlong Wang, Lei Chen, Yiwen Sun, Xinpei Wang and Junjie Ruan

College of Municipal and Environmental Engineering, Jilin Jianzhu University, Changchun 130118, China; jianlong9808@163.com (J.W.); chenlei@jlu.edu.cn (L.C.); sunyiweny101@163.com (Y.S.); wangxinpei2022@163.com (X.W.); 1835555398@163.com (J.R.)

* Correspondence: jiangbaojun.happy@163.com

Abstract: To solve the problem of the poor treatment of high concentration landfill leachate, an electro-assisted ultraviolet (UV)/zero-valent iron (ZVI) synergistic activated persulfate (PS) system was used to treat landfill leachate. The effects of PS and ZVI dosage, initial pH value, and current density on the removal efficiency of COD and NH₃-N in landfill leachate were investigated. The treatment effects of single PS, single electrochemical, UV/PS, electro-assisted ZVI activated PS, and electro-assisted ZVI/UV co-activated PS were compared. At the same time, UV-visible and three-dimensional fluorescence spectroscopy were performed on the landfill leachate before and after treatment. The results show that under the optimal conditions of initial pH = 3, the dosage of PS/12COD = 1, ZVI = 1.5 g/L, current density 62.5 mA/cm², and *t* = 6 h, most of the macromolecular organic substances such as humic acid and fulvic acid were removed. Removal efficiencies of COD, NH₃-N, and Chroma reached 81.99%, 89.90%, and 99.75%, respectively. The BOD₅/COD value increased from 0.23 to 0.46. In addition, the radical identification results showed that the degradation of COD was due to the combined action of sulfate radicals (SO₄^{•-}) and hydroxyl radicals (•OH) and that SO₄^{•-} was dominant. The combined means of synergistic activation of PS for landfill leachate treatment was significantly better than that of single means of PS activation, confirming that electrically assisted ZVI/UV synergistic activation of PS is a promising method for landfill leachate treatment.

Keywords: landfill leachate; sulfate radicals; dimensionally stable anode; synergistic activation; zero-valent iron



Citation: Jiang, B.; Wang, J.; Chen, L.; Sun, Y.; Wang, X.; Ruan, J.

Experimental Study on the Treatment of Landfill Leachate by Electro-Assisted ZVI/UV Synergistic Activated Persulfate System.

Catalysts **2022**, *12*, 768. <https://doi.org/10.3390/catal12070768>

Academic Editors: María Victoria López Ramón and Francisco José Maldonado-Hódar

Received: 1 June 2022

Accepted: 7 July 2022

Published: 11 July 2022

Publisher's Note: MDPI stays neutral with regard to jurisdictional claims in published maps and institutional affiliations.



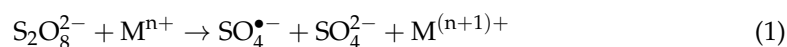
Copyright: © 2022 by the authors. Licensee MDPI, Basel, Switzerland. This article is an open access article distributed under the terms and conditions of the Creative Commons Attribution (CC BY) license (<https://creativecommons.org/licenses/by/4.0/>).

1. Introduction

Over the past decades, countries worldwide have experienced significant and rapid urbanization and industrialization, which generate vast amounts of municipal solid waste (MSW). The World Bank warns that global MSW generation will increase from 2.01 billion tons in 2016 to 3.4 billion tons by 2046 [1]. Landfill leachate is also generated continuously during the MSW landfill process due to rain and snow water washout, surface water runoff, and decomposition of organic matter [2]. It is a highly concentrated polluted wastewater containing a variety of hard-to-degrade organic pollutants, which are highly toxic. This wastewater can cause serious harm to soil and groundwater when discharged directly [3]. Currently, the sanitation industry commonly adopts a combination of biological and membrane treatment processes to treat landfill leachate [4,5]. However, this treatment method has high costs, and the landfill leachate concentrate produced after membrane treatment causes secondary pollution [6].

In recent years, the use of SO₄^{•-} based advanced oxidation processes (AOPs) for landfill leachate treatment has received much attention. This technology can efficiently degrade pollutants in landfill leachate by activating PS by single or multiple means such as

transition metal, heat, and ultraviolet light to produce highly oxidizing $\text{SO}_4^{\bullet-}$ [7], with the following reaction mechanism [8,9].



UV/ Fe^{2+} co-activation of PS with high activation efficiency and mild reaction conditions, which is relatively environmentally friendly and economical, has become one of the most commonly used methods for activating PS [10,11]. However, it is difficult to regenerate Fe^{2+} during the reaction process, and the continued addition of iron sources will increase the cost and generate a large amount of iron sludge. This drawback dramatically limits the application of this method [12].

However, this problem can be effectively solved by using ZVI in this system instead of Fe^{2+} activation of PS, in combination with an electrochemical oxidation reaction. ZVI can gradually release Fe^{2+} under acidic conditions, and Fe^{3+} can also be reduced to Fe^{2+} on the surface of ZVI, according to (4) and (5) [13,14]. Furthermore, excessive Fe^{2+} consumption of $\text{SO}_4^{\bullet-}$ at the beginning of the reaction is avoided, according to Equation (6) [15]. Fe^{2+} can also be continuously generated on the cathode surface when combined with electrochemical oxidation during the reaction, according to Equation (7) [16].



Studies on landfill leachate treatment using the electro-assisted ZVI/UV synergistic activation PS method have not been reported. In this study, to evaluate the treatment efficacy of electro-assisted ZVI/UV synergistic activation PS on landfill leachate and to determine the optimal reaction conditions, the effects of operating conditions such as initial pH, PS and ZVI dosage, and current density on the removal of pollutants and improvement of biodegradability properties in landfill leachate were investigated. The treatment effects of the synergistic activation system were compared with those of the single activation system. In addition, UV-visible and 3D fluorescence spectroscopy were performed on the landfill leachate before and after treatment to understand the conversion of organic pollutants in the landfill leachate.

2. Results and Discussion

2.1. Compare Treatment Processes and Analyze Synergistic Effects

To verify the advantages and synergistic effects of the electro-assisted ZVI/UV combined activated PS system for landfill leachate treatment, 5 groups of systems were set up in this study for comparison experiments: single electrochemical oxidation system, single PS system, UV/PS system, electro-assisted ZVI/PS system, and electro-assisted ZVI/UV combined activated PS system for landfill leachate treatment under the same reaction conditions, respectively.

As shown in Figure 1a, each system can remove COD and $\text{NH}_3\text{-N}$ from landfill leachate, but there are significant differences in the removal effectiveness of each system. The removal rates of COD for the single PS system, UV/PS system, and single electrochemical system were 2.15%, 6.79%, and 14.96%. In the treatment process of the single PS system, the complex composition of leachate pollutants, containing a large number of hard-to-degrade organic pollutants, and the low reaction rate of PS directly with organic contaminants, led to the poor treatment effect of PS alone. Under UV light conditions,

the O-O absorption energy of PS breaks to generate $\text{SO}_4^{\bullet-}$ and radicals participate in the reaction to help enhance the treatment effect. However, in the treatment process of the UV/PS system, landfill leachate's high turbidity and chroma may prevent UV from penetrating the activation PS of landfill leachate, so the treatment effect enhancement is not apparent. During the treatment of landfill leachate by electrochemical oxidation alone, hydroxyl radicals generated by hydrolysis on the surface of the shape-stabilized anode (DSA) are tightly adsorbed on the anode surface according to Equation (8), resulting in limited removal of pollutants [17]. In addition, oxygen evolution on the anode surface can further reduce the efficiency of contaminant treatment [18].

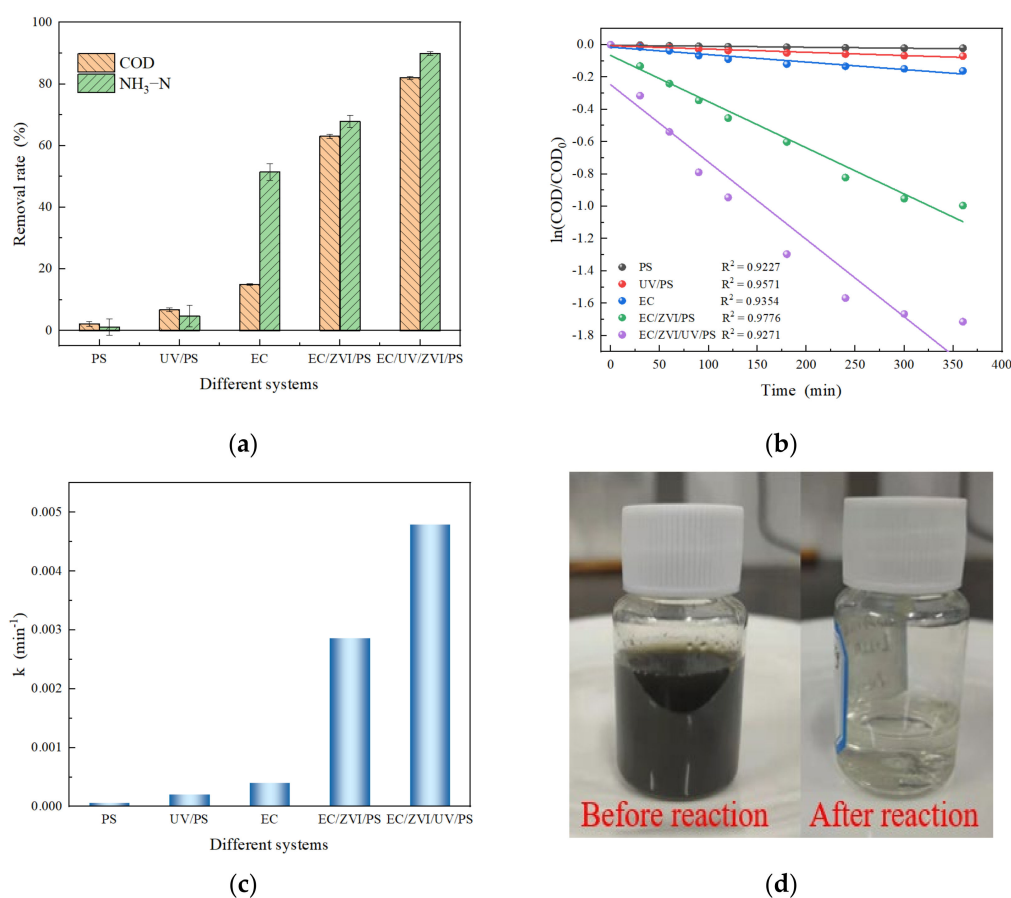
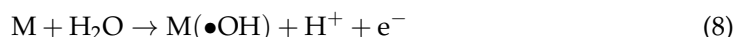


Figure 1. (a) Removal efficiencies of COD and NH₃-N from landfill leachate by different systems. (b) Pseudo-first-order kinetic models for COD removal in different systems. (c) The k of COD under different reaction systems. (d) The state changes of the leachate before and after the treatment of the electro-assisted ZVI/UV combined activated PS system. (Initial pH: 3.0; PS/12COD ratio: 1; ZVI dosage: 1.5 g/L; current density: 62.5 mA/cm²; reaction time: 6 h).

The COD removal rate increased to 63.04%, and the NH₃-N removal rate increased to 71.84% during the electro-assisted ZVI activated PS for landfill leachate treatment. This was due to the effective activation of PS by Fe²⁺ in the system to produce $\text{SO}_4^{\bullet-}$, which led to the effective removal of pollutants. The highest COD and NH₃-N removal rates of 81.99% and 89.90%, respectively, were achieved in the combined electrically assisted ZVI/UV activated PS system. Figure 1d shows the difference in landfill leachate status before and after treatment with the electro-assisted ZVI/UV combined activated PS system. Obviously, the combined use of ZVI and UV can reduce the activation energy of PS so that it can be activated more effectively. This proves that the combined electrically assisted

ZVI/UV activated PS system has apparent advantages in treating landfill leachate. We can also reasonably infer that the combined UV and ZVI activation PS has synergistic effects.

For the kinetic analysis, the degradation efficiency of COD was hypothesized by the first-order kinetic reaction, according to Equation (9). The results are shown in Figure 1b, where the COD kinetic model for $\text{SO}_4^{\bullet-}$ degradation follows pseudo-first-order kinetics.

$$-\frac{dC}{dt} = kC \leftrightarrow \ln \frac{C_t}{C_0} = -kt \quad (9)$$

where k is the reaction rate constant, C is the COD concentration in the water sample, and C_0 and C_t denote the COD concentration in the water sample at moments 0 and t , respectively.

Figure 1c shows that the reaction rate constants for each system to degrade COD in landfill leachate are: $k_{\text{PS}} = 0.000004 \text{ min}^{-1}$, $k_{\text{UV/PS}} = 0.00002 \text{ min}^{-1}$, $k_{\text{EC}} = 0.00005 \text{ min}^{-1}$, $k_{\text{EC/ZVI/PS}} = 0.00286 \text{ min}^{-1}$, and $k_{\text{EC/ZVI/UV/PS}} = 0.00479 \text{ min}^{-1}$. Combining ZVI and UV to activate PS for landfill leachate treatment improved the reaction rate and shortened the system's reaction time. To further verify the synergy of UV and ZVI combined with activated PS, the degree of performance synergy was quantified according to Equation (10) [19].

$$S(\%) = \frac{k_{\text{combined}} - \sum_i^n k_i}{k_{\text{combined}}} \times 100 \\ = \frac{k_{\text{EC/ZVI/UV/PS}} - (k_{\text{UV/PS}} + k_{\text{EC/ZVI/PS}})}{k_{\text{combined}}} \times 100 \quad (10)$$

where $S = \begin{cases} > 0, \text{ synergistic effect} \\ = 0, \text{ cumulative effect} \\ < 0, \text{ competitive effect} \end{cases}$.

We calculated the degree of a synergy of ZVI and UV co-activation PS as 38.54%, indicating a practical synergistic effect of the co-activation process rather than an accumulation phenomenon.

2.2. Optimum Parameters of Landfill Leachate Treatment

2.2.1. Effects of Initial pH Value

As we all know, pH control is essential in water treatment. Many reports have shown that $\text{SO}_4^{\bullet-}$ based AOPs operate better under acidic conditions [20]. To evaluate the effect of initial pH value on the removal rate of COD, $\text{NH}_3\text{-N}$, and chroma from leachate, experiments were conducted at initial pH values of 1.0, 3.0, 5.0, 7.0, and 9.0. According to Figure 2a, the initial pH value's effect on chroma's removal rate was relatively small. The removal rates of COD and $\text{NH}_3\text{-N}$ gradually increased as the initial pH value decreased from 9.0 to 3.0. When the pH value was 3.0, the removal rates of COD, $\text{NH}_3\text{-N}$, and chroma reached the maximum, which were 81.99%, 89.90%, and 99.75%, respectively. To understand the kinetics of COD degradation at different initial pH values, the degradation data of COD at different pH value conditions were fitted. Figure 2b shows that COD degradation at different pH conditions conforms to pseudo-first-order kinetics, and the reaction rate constant k decreases with increasing initial pH value, which is consistent with the dependence of COD removal rate on the initial pH value shown in Figure 2a.

In the present system, ZVI needs to be dissolved from the surface of iron powder under strongly acidic conditions, according to Equation (4), and the resulting ferrous ions react rapidly with PS to form $\text{SO}_4^{\bullet-}$, according to Equation (1). PS is decomposed under strongly acidic conditions, catalyzed by acid to produce $\text{SO}_4^{\bullet-}$, according to Equations (11) and (12) [21]. However, at higher pH, on the one hand, the concentration of dissolved iron ions decreases, and the activation PS process is slowed down, which is the main reason for the decline in the degradation efficiency of pollutants. On the other hand, at $\text{pH} > 3$, iron ions generate $\text{Fe}(\text{OH})_n$ ($n = 2, 3$) complexes, which can hinder the production of $\text{SO}_4^{\bullet-}$ [22]. In addition, the scavenging effect of carbonates and bicarbonates on reactive

oxygen species (ROS) is intensified under weakly acidic and neutral conditions, leading to a decrease in oxidation efficiency [23].

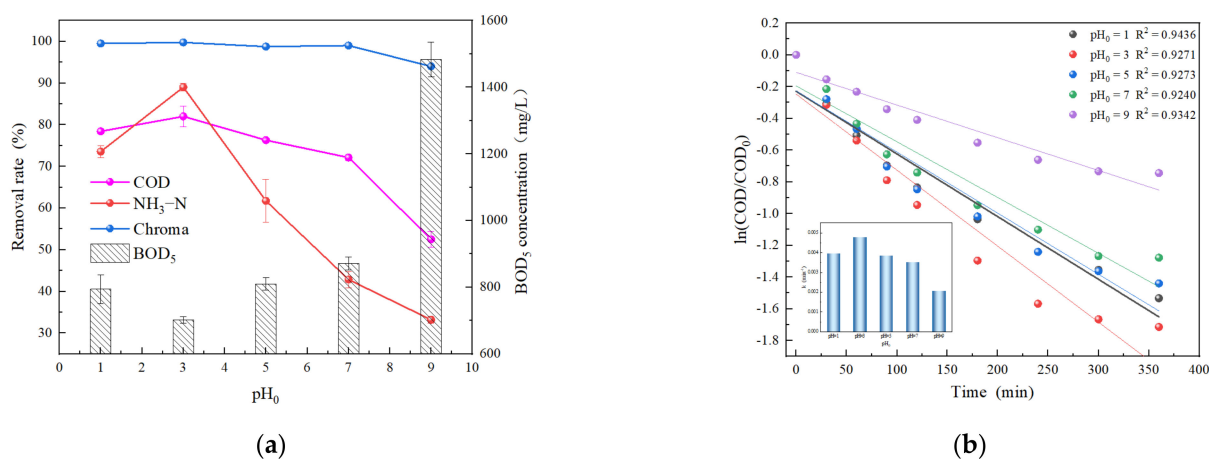
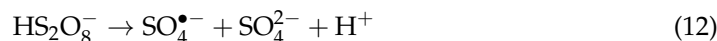
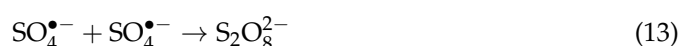
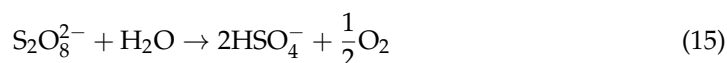


Figure 2. (a) Effects of initial pH on COD, NH₃-N, chroma removal rate, and BOD₅ content. (b) Pseudo-first-order kinetic models of COD degradation at different initial pH values. (Initial pH: 3.0; PS/12COD ratio: 1; ZVI dosage: 1.5 g/L; current density: 62.5 mA/cm²; reaction time: 6 h).

When the initial pH decreased to 1.0, the removal rates of COD and NH₃-N did not continue to increase with the decrease of pH but decreased to 78.42% and 73.56%. This may be due to the rapid decomposition of PS under the multiple activations of strong acid, ZVI, and UV to produce excessive SO₄^{•−} in a short time, resulting in the self-scavenging reaction of SO₄^{•−} according to Equation (13). Based on the above results, subsequent experiments were conducted at an initial pH of 3.0.



During the experiments, we also found that the pH of the system effluent decreased to varying degrees. This is due to the acidification that occurs during the treatment process, the formation of hypochlorous acid by reactions such as PS hydrolysis, and the accumulation of small-molecule organic acids such as carboxylic acids as shown in Equations (14) and (15) [24].



2.2.2. Effects of PS Dosage

In SO₄^{•−} based on AOPs, the amount of PS dosing determines the SO₄^{•−} content in the system and the reaction efficiency in the treatment process, so PS dosing is one of the critical control factors [25]. Based on the redox ratio calculation, it is known that 12 mol of persulfate is theoretically required to oxidize 1 mol of COD completely, so this experiment was conducted by setting the PS dosage as PS/12COD = 0, 0.25, 0.5, 0.75, 1, 1.25, respectively. The effects of PS concentration on the removal of COD, NH₃-N, chroma, and BOD₅ at an initial pH = 3.0, a ZVI dosage = 1.5 g/L, and a current density = 62.5 mA/cm² and a running time = 6 h are shown in Figure 3a. As seen in the figure, the removal rates of COD, NH₃-N, and chroma increased gradually as the PS concentration increased from PS/12COD = 0.25 to PS/12COD = 1.0. Still, the removal

rates of COD and NH₃-N decreased significantly when the PS concentration increased to PS/12COD = 1.25. A similar trend of kinetic reaction rate constant *k* for COD degradation can be seen in Figure 3b. *k* values ranged from 0.00175 to 0.00479 min⁻¹ when the PS dosage was increased from PS/12COD = 0.25 to PS/12COD = 1.0; when the PS dosage was further increased to PS/12COD = 1.25, the *k* values decreased to 0.00435 min⁻¹.

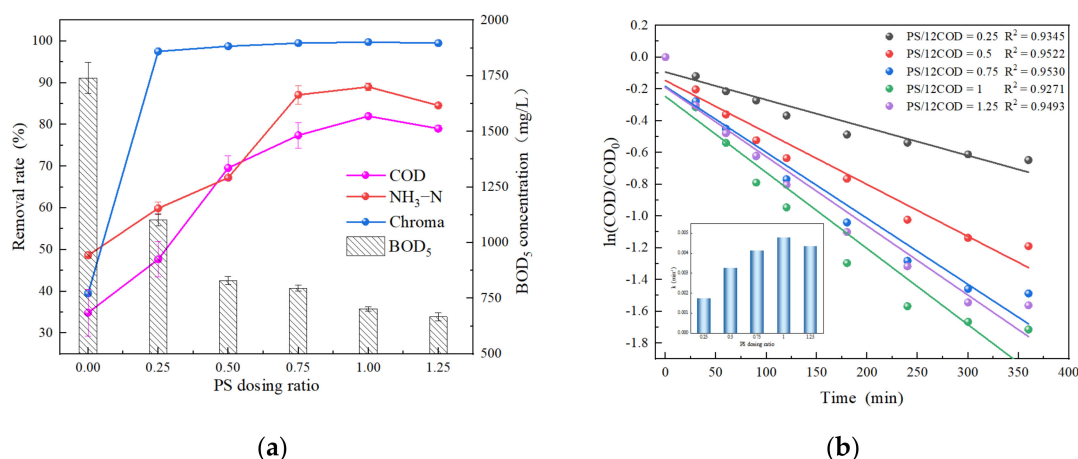
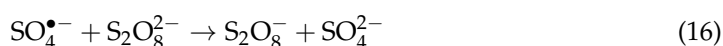


Figure 3. (a) Effects of PS dosage on COD, NH₃-N, chroma removal rate, and BOD₅ content. (b) Pseudo-first-order kinetic models of COD degradation at different PS dosage levels. (Initial pH: 3.0; PS/12COD ratio: 1; ZVI dosage: 1.5 g/L; current density: 62.5 mA/cm²; reaction time: 6 h).

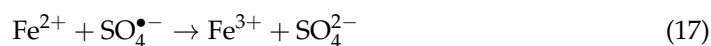
Generally, the higher the SO₄^{•-} content, the more organic matter and NH₃-N are removed, but in this study, when the PS concentration reached PS/12COD = 1.25, the removal rate decreased instead of rising. This is because when the concentration of SO₄^{•-} is too high, SO₄^{•-} will not only have a quenching effect with PS, according to Equation (16), but also SO₄^{•-} will perform self-scavenging according to Equation (13) [26,27]. This is the main reason PS utilization efficiency cannot reach 100% when PS degrades organic pollutants in leachate. The COD and NH₃-N removal rates still reached 34.88% and 48.65%, respectively, when no PS was added, probably because of the contribution of electrochemical oxidation and iron coagulation and precipitation.



It can be seen from Figure 3a that the BOD₅ content decreased with the increase in PS concentration. This is mainly due to 2 reasons: (1) the oxidative removal of organic pollutants and (2) the increase in reagent residues affecting microbial degradation. Therefore, the optimal dosage of PS in this study was PS/12COD = 1.

2.2.3. Effects of ZVI Dosage

In the electrically assisted ZVI/UV synergistic activated PS system, ZVI can be gradually converted to Fe²⁺ and activate PS to produce sulfate radicals on the one hand; on the other hand, it plays a considerable role in the subsequent coagulation process, so the amount of ZVI dosing has an important influence on this experiment [28]. 5 sets of experiments with different dosing amounts were tested to investigate the effects of ZVI dosing. Figure 4 shows that when no ZVI was added, the system had a minimal impact on removing COD, chroma, etc. When the ZVI dosage was increased from 0.5 g/L to 1.5 g/L, the kinetic constant of COD removal increased from 0.00241 min⁻¹ to 0.00479 min⁻¹, and the COD removal rate increased from 58.77% to 81.99%. The NH₃-N and chroma removal rates increased from 75.89% and 90% to 89.02% and 99.75%, respectively.



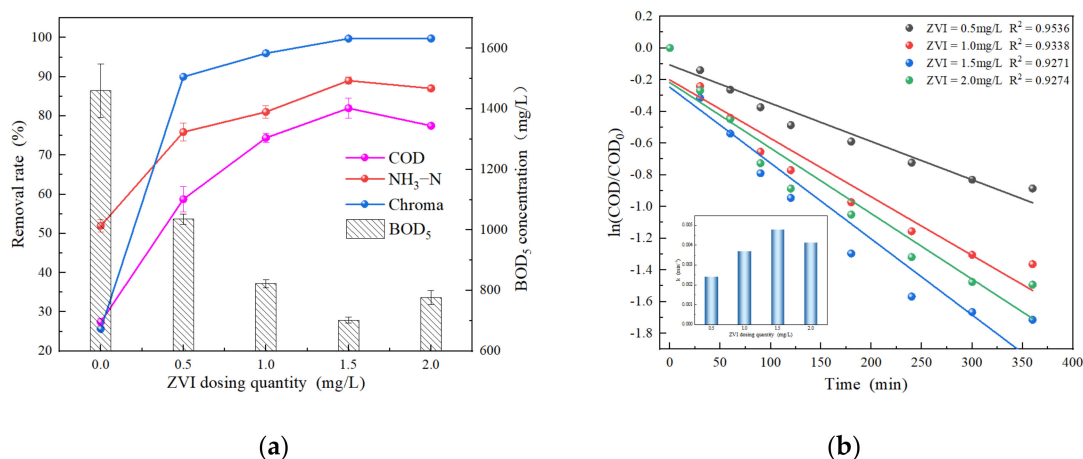


Figure 4. (a) Effects of ZVI dosing on COD, NH₃-N, chroma removal, and BOD₅ content. (b) Pseudo-first-order kinetic models of COD degradation at different ZVI dosage levels. (Initial pH: 3.0; PS/12COD ratio: 1; ZVI dosage: 1.5 g/L; current density: 62.5 mA/cm²; reaction time: 6 h).

In the follow-up study, ZVI dosage was controlled at 1.5 g/L to achieve a better treatment effect.

2.2.4. Effects of Current Density

To investigate the effects of current density on the treatment effect of landfill leachate, 5 sets of experiments were conducted with different current densities, 0, 12.5, 37.5, 62.5, and 87.5 mA/cm². From Figure 5a, it can be seen that when the current density was increased from 12.5 mA/cm² to 62.5 mA/cm², the NH₃-N and chroma removal rates increased from 74.66% and 96% to 89.02%, and 99.75%, respectively, and the COD removal rate increased from 61.32% to 81.99%. The corresponding rate constants increased from 0.00264 min⁻¹ to 0.00479 min⁻¹ (Figure 5b).

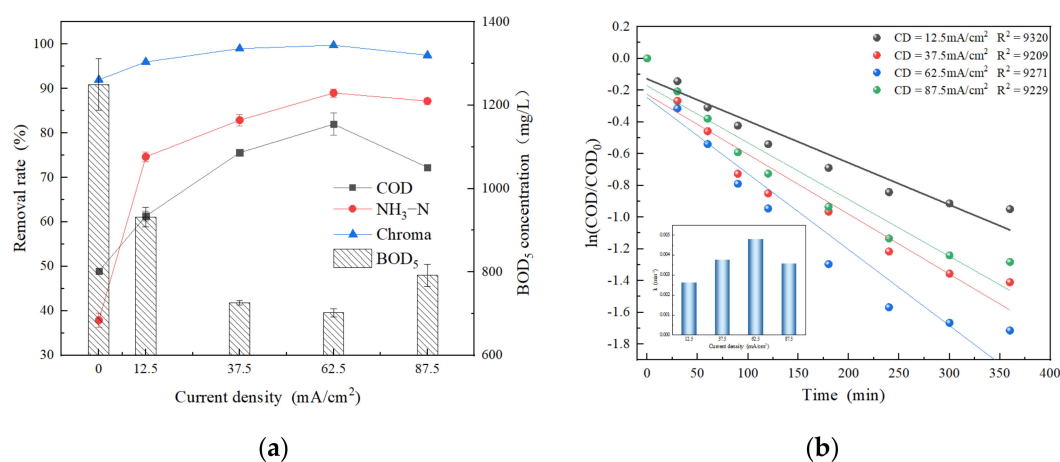


Figure 5. (a) Effects of current density on COD, NH₃-N, chroma removal, and BOD₅ content. (b) Pseudo-first-order kinetic models of COD degradation at different current densities. (Initial pH: 3.0; PS/12COD ratio: 1; ZVI dosage: 1.5 g/L; current density: 62.5 mA/cm²; reaction time: 6 h).

Increasing the current density will speed up the electron transfer rate and allow faster reduction of Fe³⁺ to Fe²⁺, favoring the PS decomposition to produce sulfate radicals. However, further increasing the current density will cause side reactions such as oxygen and hydrogen evolution to be enhanced as well, according to Equations (18) and (19) [29]. The enhancement of the side reactions inhibits the primary reaction of Fe³⁺ reduction to Fe²⁺ and weakens the activation process of PS by Fe²⁺. This is the main reason why

the COD removal rate and rate constant decreased even though the current density was increased to 87.5 mA/cm².



2.2.5. Effects of Reaction Time

The effects of reaction time were examined to investigate better the ability of electrically assisted ZVI/UV/PS to treat leachate and determine the optimal treatment time. The experimental control conditions were: the initial pH was 3.0, the PS dosage was PS/12COD = 1.0, the ZVI dosage was 15 g/L, and the current density was 62.5 mA/cm². Figure 6 shows that the COD and NH₃-N removal rates increased rapidly with the reaction time in the first 2 h. After 2 h, the reaction rate gradually slowed down, and the highest NH₃-N removal rate was achieved in the 5th hour of the reaction, while the highest COD removal rate was achieved in the 6th hour. After 6 h, the reaction time continued to increase, and the removal rate stabilized. This indicates that the leachate treatment with the electrically assisted ZVI/UV synergistic activated PS system stopped after 6 h.

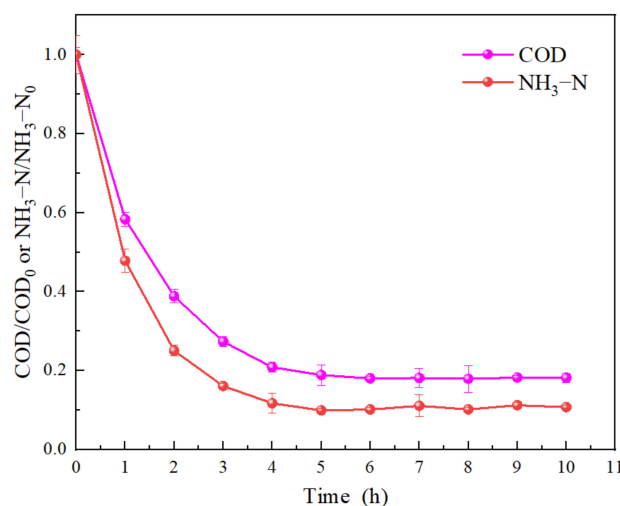


Figure 6. Variation of COD and NH₃-N removal rate with reaction time. (Initial pH: 3.0; PS/12COD ratio: 1; ZVI dosage: 1.5 g/L; current density: 62.5 mA/cm²; reaction time: 6 h).

Similar studies have shown that as the reaction time increases, the pollutants are exposed to more and more radicals and therefore are affected more and more [30]. Furthermore, most contaminants are degraded and removed at the early stage of the reaction because at the beginning of the response, both the oxidant concentration and the catalyst activity are the highest, and the mutual reaction rate between the two is naturally the fastest.

2.3. Analysis of Water Quality Characteristics

2.3.1. UV-Vis Spectrum Analysis

The landfill leachate before and after treatment was diluted 20 times and scanned by UV-Vis spectroscopy to understand the degradation of aromatic compounds, and the results are shown in Figure 7. As shown in the figure, there is no apparent characteristic peak in the spectrogram of raw landfill leachate. The absorbance decreases gradually with the increase of wavelength; the absorbance of treated leachate is more extensive in the range of 200–220 nm. The absorbance starts to fall sharply at 220 nm, and the absorbance drops to 0 at 386 nm.

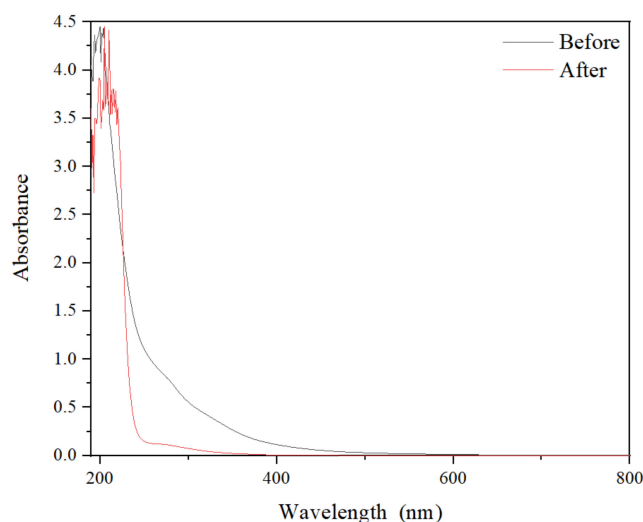


Figure 7. UV-Vis spectra of landfill leachate before and after treatment. (Initial pH: 3.0; PS/12COD ratio: 1; ZVI dosage: 1.5 g/L; current density: 62.5 mA/cm²; reaction time: 6 h).

The inability to observe significant peaks in the UV-Vis spectrogram for raw water is attributed to the complexity of organic matter in landfill leachate. It is well known that a macromolecular DOM has a higher content of aromatic and unsaturated co-choked double bond structures than a small molecule DOM, which has a higher UV absorption intensity per mole after 230 nm wavelength [31]. The unsaturated bonds and aromatic structures of a large amount of macromolecular DOM are destroyed by $\text{SO}_4^{\bullet-}$ after landfill leachate treatment and converted into small molecule DOM. Absorbance at wavelength 254 nm can characterize the content of compounds with unsaturated carbon-carbon bonds, including aromatic compounds, and absorbance at wavelength 280 nm can characterize the aromaticity and hydrophobicity of DOM [32]. In this experiment, the absorbance of treated landfill leachate decreased from 1.04 to 0.13 at 254 nm and from 0.767 to 0.108 at 280 nm. This implies a significant degradation of humic substances in landfill leachate and a considerable decrease in the aromaticity and hydrophobicity of DOM. E_{253}/E_{203} can indicate the number and type of substituents on the aromatic ring. The significant reduction of E_{253}/E_{203} in the treated leachate demonstrates that the organic matter with an aromatic ring structure with -COOH, -OH, and -C-O as substituents were effectively removed during the treatment [33]. The absorbance of the treated landfill leachate exceeded that of the raw water at wavelengths 200–225, which may be due to the introduction of inorganic anions such as sulfate due to the addition of PS inorganic anions having a more significant absorbance here.

2.3.2. 3D Fluorescence Spectrum Analysis

3D fluorescence spectroscopy scans were performed by diluting the landfill leachate before and after treatment 50 times and were used to evaluate the conversion of dissolved organic pollutants in the landfill leachate during the electro-assisted ZVI/UV synergistic activation PS treatment. The results are shown in Figure 8. Three fluorescence peaks can be observed in Figure 8a, and according to a previous report [34], fluorescence peak A (Ex/Em = 245/457 nm) is for fulvic acid-like substances, fluorescence peak B (Ex/Em = 320/407 nm) is for humic acid-like substances, and fluorescence peak C (Ex/Em = 280/338 nm) is for soluble microbial metabolism by-products. The most vigorous fluorescence intensity of peak A exceeded 5800 Au, indicating the highest content of fulvic acid-like substances. Fulvic acids, soluble microbial metabolism by-products, and humic acids are all refractory pollutants [35], which explains the low biodegradability of raw water. Figure 8b shows that the fluorescence intensities of all three fluorescence peaks were substantially weakened, and the fluorescence intensity of peak A decreased by 97%,

which indicated that the system was effective in removing fulvic acid-like substances, and soluble microbial metabolic by-products, and humic acid-like substances.

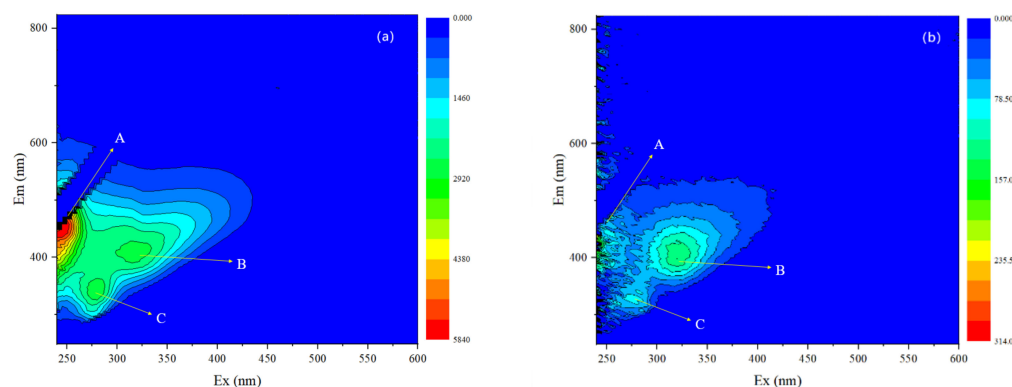


Figure 8. 3D fluorescence spectra of landfill leachate before (a) and after (b) treatment. (Initial pH: 3.0; PS/12COD ratio: 1; ZVI dosage: 1.5 g/L; current density: 62.5 mA/cm²; reaction time: 6 h).

2.4. Changes in Biodegradability

As shown in Figure 9, BOD₅/COD increased with increasing reaction time. This is in contrast to the study by Fatemeh et al. [36], in which the leachate was low-age landfill leachate with a BOD₅/COD ratio greater than 0.6, and the ratio decreased after purification. However, this study's initial BOD₅/COD ratio was 0.23, indicating that the landfill leachate was more mature and had a lower content of biodegradable substances. After 6 h treatment, the BOD₅/COD ratio increased to 0.46, and the biodegradability improved significantly.

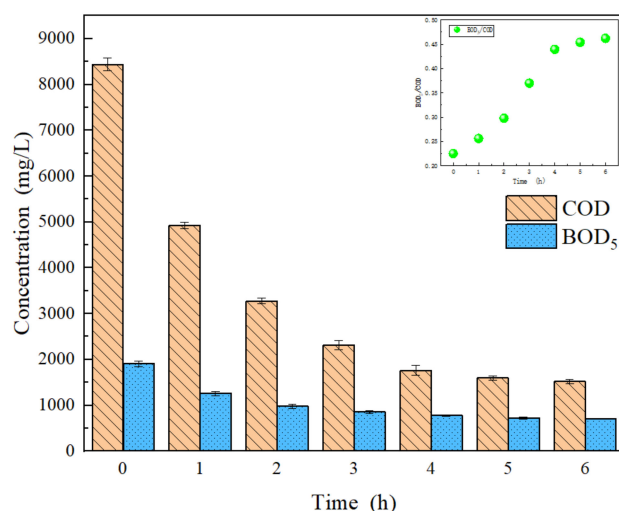


Figure 9. Changes in biodegradability with reaction time. (Initial pH: 3.0; PS/12COD ratio: 1; ZVI dosage: 1.5 g/L; current density: 62.5 mA/cm²; reaction time: 6 h).

In mature landfill leachate, a large proportion of the pollutants are hard-to-biodegrade compounds (the main component of COD). The electrically assisted ZVI/UV synergistic activated PS system can remove most of the refractory pollutants. Macromolecular organic substances such as fulvic acid and humic acid were degraded into smaller molecular organic substances. The aromaticity and phenyl compound content was reduced, greatly facilitating the subsequent biological treatment.

2.5. Identification of Radicals

To determine the main radical species for degrading COD in landfill leachate, classical scavengers such as benzoquinone (BQ), anhydrous ethanol (EtOH), and tert-butanol (TBA)

were used for radical quenching experiments. In the radical quenching experiments, EtOH showed sound quenching effects on both $\text{SO}_4^{\bullet-}$ ($k = 1.6 \times 10^7 \sim 7.7 \times 10^7 \text{ M}^{-1}\text{s}^{-1}$) and $\bullet\text{OH}$ ($k = 1.2 \times 10^9 \sim 2.8 \times 10^9 \text{ M}^{-1}\text{s}^{-1}$). TBA reacts with $\bullet\text{OH}$ ($k = 3.8 \times 10^9$ to $7.6 \times 10^9 \text{ M}^{-1}\text{s}^{-1}$) at a high rate, unlike EtOH, which reacts with $\text{SO}_4^{\bullet-}$ ($k = 4.0 \times 10^5$ to $8.1 \times 10^5 \text{ M}^{-1}\text{s}^{-1}$) at a slower pace [37], and BQ readily reacts with superoxide radicals ($\text{O}_2^{\bullet-}$) ($k = 9.6 \times 10^8 \text{ M}^{-1}\text{s}^{-1}$) [38]. Excess scavengers were added to the system separately to identify the radicals participating in the degradation of COD. Figure 10 shows the results of the radical scavenging experiments. It can be seen that the addition of BQ did not affect the removal of COD at different pH conditions, in contrast to the significant inhibition of COD degradation at different pH conditions by the addition of EtOH. The addition of TBA decreased the removal of COD, and the inhibition effect was significantly more potent at pH = 9 than at pH = 3, from 81.99% and 52.51% to 80.59% and 45.2%, respectively.

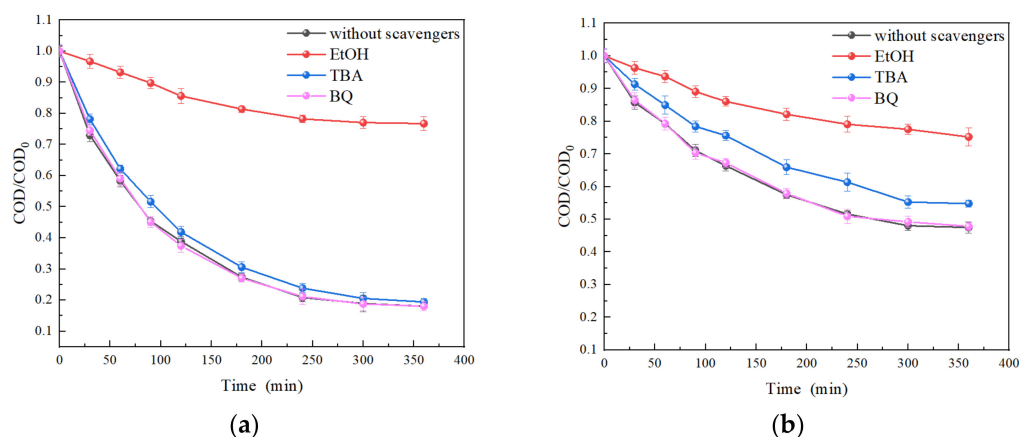


Figure 10. Radicals' contribution in electrically assisted ZVI/UV synergistic activated PS system. Reaction conditions: PS/12COD ratio = 1; ZVI dosage = 1.5 g/L; current density = 62.5 mA/cm², reaction time = 6 h; molar ratio COD: scavenger = 1:50. Initial pH = 3.0 (a). Initial pH = 9.0 (b).

Through the experimental results, it is evident that there is no $\text{O}_2^{\bullet-}$ involved in the degradation of COD in the system, and the degradation of COD mainly relies on the joint action of $\text{SO}_4^{\bullet-}$ and $\bullet\text{OH}$. Overall, $\text{SO}_4^{\bullet-}$ occupies a prominent dominant role in the degradation reaction of COD. The contribution of $\bullet\text{OH}$ to the degradation of COD under acidic conditions was limited. This agrees with the results obtained by Hannah et al. [39], who confirmed that at pH < 7, $\text{SO}_4^{\bullet-}$ is the dominant radical. Zhang et al. [40] found that $\bullet\text{OH}$ is readily generated at higher pH. Therefore, the contribution of $\bullet\text{OH}$ to COD degradation increases under alkaline conditions.

2.6. Energy Consumption

Electrical energy consumption in the electrically assisted ZVI/UV synergistic activated PS system is a non-negligible factor. In this study, the primary energy inputs to the system were the DC power supply and the UV lamp. To further investigate the energy consumption efficiency of the applied system for COD removal, the specific electrical energy consumption (SEEC) was calculated according to Equation (20) [41].

$$\text{SEEC} \left(\frac{\text{kWh}}{\text{kg COD}} \right) = \frac{\sum P \times t}{(\text{COD}_0 - \text{COD}) \times V} \quad (20)$$

where P is the input electrical energy required for the system (kW), t is the required treatment time (h), and V is the volume of landfill leachate treated (L).

According to previous studies, using advanced oxidation technology, an energy-consuming suitable process requires an electrical energy consumption value of less than 100 kWh/kg COD for COD degradation [42]. For the system developed in this study, the

energy consumption was calculated to be 0.52 kWh/kg COD, which is much lower than this evaluation criterion.

Table 1 summarizes the electrical power consumption of AOPs for COD removal from leachate. It can be seen that the energy efficiency of the electrically assisted ZVI/UV synergistic activation PS system is higher because it generates more sulfate radicals and is more efficient for COD removal. Table 1 shows that although the removal efficiency of W.-J et al. was as high as 87% [43], their electrical power consumption (91.9 kWh/kg COD) was much higher than that of the present system (0.52 kWh/kg COD).

Table 1. Comparison of specific electrical energy consumption (SEEC) under the different systems for treating the leachate.

Treatment Process	Leachate COD Concentration (mg/L)	Optimal Conditions	Removal Efficiency (%)	Energy Consumption (kWh/kgCOD)	References
Electrically assisted ZVI/UV synergistic activation PS system	48,440	PS/12COD ratio: 1; ZVI dosage: 1.5 g/L; The current density: 62.5 mA/cm ² , reaction time: 6 h; initial pH: 3.0	81.99	0.52	This work
Micro-waved system coupled Fenton	8900 + 120	Fe ²⁺ = 0.04 M, H ₂ O ₂ = 0.075 M, pH = 3.1, V = 100 mL and reaction time = 36 min	61	833.34	[41]
Electro-oxidation + PS oxidation	1281	I = 80 mA, [PDS] = 75 mM, [Fe ³⁺] = 15 mM, V = 0.15 L and reaction time = 120 min	87	91.9	[43]
Electro-Fenton	1625	I = 200 mA, pH = 3, aeration rate = 0.32 L/min, [Fe ²⁺] = 0.8 mM, V = 800 mL and reaction time = 2 h	74.7	5.76	[44]
Electro/Fe ⁰ /H ₂ O ₂	2500	pH ₀ : 2.0, Fe ⁰ loading: 1.745 g/L, H ₂ O ₂ dosage: 0.187 mol/L, current density: 20.6 mA/cm ² , inter-electrode gap: 1.8 cm, treatment time: 2 h	70.1	8.12	[40]
Electrochemical oxidation	6000	4% NaCl, solution pH 5.5, applied voltage 20 V, temperature: 80 °C, FeSO ₄ ·7H ₂ O: 4 g/L, input rate of leachate: 60 mL/min, treatment time: 5 h	41.6	4.29	[45]
Electrochemical oxidation	780	pH 8.2, current: 2 A, temperature: 50 °C, inter-electrode gap: 0.5 cm, treatment time: 3 h	<160 mg/L	145.16	[46]
Electro-coagulation	10,000 ± 200	I = 3.5 A, pH = 7, V = 0.5 L and reaction time = 20 min	57.4	–	[47]

3. Materials and Methods

3.1. Materials

3.1.1. Chemical Reagents

Sodium persulfate (Na₂S₂O₈), zero-valent iron (ZVI), sulfuric acid (H₂SO₄), sodium hydroxide (NaOH), ferrous ammonium sulfate (Fe(NH₄)₂·(SO₄)₂·6H₂O), potassium dichromate (K₂Cr₂O₇), mercury sulfate (HgSO₄), potassium hydrogen phthalate (KHC₈H₄O₄), mercury iodide (HgI₂), potassium persulfate (K₂S₂O₈), potassium dihydrogen phosphate (KH₂PO₄) and other reagents were purchased from Sinopharm Chemical Reagent Co., Ltd. (Shanghai, China). All chemical reagents were analytical grade reagents in this experiment, and the water used was deionized.

3.1.2. Landfill Leachate

The used landfill leachate water samples were taken from a landfill in Shuangliao City, Jilin Province, China, and stored in a refrigerator at 4 °C after retrieval. The water samples

were dark black and emitted a foul odor; their leading water quality indicators are shown in Table 2.

Table 2. Landfill leachate characteristics.

Parameter	Range	Average
COD (mg/L)	8280~8570	8440
BOD ₅ (mg/L)	1832~1950	1901
BOD ₅ /COD	0.22~0.23	0.23
NH ₃ -N (mg/L)	2269~2497	2384
pH	7.64~7.82	7.75
SS (mg/L)	17,390~18,560	17,873
TN (mg/L)	2633~2809	2699
TP (mg/L)	25.3~29.4	27.50
Chroma (times)	3200	3200

3.2. Experimental Procedures

The experimental device consists of a UV lamp, a DC power supply, a magnetic stirrer, an electrolytic cell, and an isolation box. The electrolytic cell is made of Plexiglas with 10 cm × 6 cm × 12.5 cm, and the electrodes are fixed in the cell at 1.5 cm intervals. The anode was Ti/IrO₂-RuO₂-TiO₂, and the cathode was pure titanium, measuring 10 cm × 10 cm. The UV lamp was fixed above the isolation chamber, 20 cm from the top of the electrolyzer.

Before each test, the UV lamp was turned on to preheat for 30 min. Set the output current density of the DC power supply (0, 12.5, 37.5, 62.5, and 87.5 mA/cm²). After stabilization by UV light, 200 mL of landfill leachate was placed in an electrolyzer, and the initial pH of the landfill leachate was adjusted using concentrated H₂SO₄ and concentrated NaOH (1.0, 3.0, 5.0, 7.0, and 9.0). Then, a predetermined dose of Na₂S₂O₈ (PS/12COD = 0, 0.25, 0.5, 0.75, 1.0, 1.25) and ZVI (0, 0.5, 1.0, 1.5 and 2.0 mg/L) was added to the leachate. Immediately afterward, the electrolytic cell was placed on a magnetic stirrer, and the experiment was turned on with DC power. During the experiment, a 10 mL water sample was taken at predetermined intervals, and the pH value was adjusted to above 8.20 immediately after removing the water sample. The water samples were centrifuged at 2000 r/min for 15 min using a centrifuge, and the supernatant was taken to determine its water quality index. Each group of experiments was repeated 3 times, and the final results were reported as the average value.

3.3. Analysis Method

The testing methods of water quality indexes in the experiments were all based on the “National Environmental Protection Standard of the People’s Republic of China”, and the specific testing methods are shown in Table 3.

Table 3. Detection method.

Indicators	Method	Standard Number
COD	Dichromate process	HJ 828–2017
NH ₃ -N	Nessler’s reagent spectrophotometry	HJ 5,352,009
BOD ₅	Dilution and seeding method	HJ 505–2009
Chroma	Dilution level method	HJ 1182–2021
pH	PHS-3C PH meter	—
3D fluorescence spectrum	3D fluorescence spectrometer	—
Uv-visible spectrum	Uv-visible spectrophotometer	—

4. Conclusions

- (i) The treatment efficacy of the electro-assisted ZVI/ UV synergistic activated PS system was investigated in experiments to treat landfill leachate. The results showed that under the optimal conditions (Initial pH: 3.0; PS/12COD ratio: 1; ZVI dosage: 1.5 g/L; current density: 62.5 mA/cm²; reaction time: 6 h), the removal rates of COD, NH₃-N

and chroma reached 81.99 %, 89.90 % and 99.75 %, respectively, and the BOD5/COD ratio increased from 0.23 to 0.46.

- (ii) The degradation of COD is caused by the combined action of sulfate radicals and hydroxyl radicals. Sulfate radicals dominate, and the contribution of hydroxyl radicals increases under alkaline conditions.
- (iii) UV-Vis and 3D fluorescence spectroscopy showed that most large-molecule organic substances such as humic acid and fulvic acid in the landfill leachate were degraded to small-molecule organic substances.
- (iv) Comparative experiments showed that the UV and ZVI synergistic activated PS was significantly more effective in removing organic pollutants from high concentration landfill leachate than the single activation system.

Author Contributions: B.J.: Conceptualization, Funding Acquisition, Supervision. J.W.: Investigation, Experimental Design, and Writing. L.C.: Methodology, Supervision. Y.S. and X.W.: Data curation, Formal Analysis, and Investigation. J.R.: Writing—Review and Editing. All authors have read and agreed to the published version of the manuscript.

Funding: This research received no external funding.

Data Availability Statement: Detailed data for this experiment are available online at <https://note.youdao.com/s/ZRW93jSV>, (accessed on 1 May 2022).

Acknowledgments: The authors acknowledge the support of the Key Laboratory of Songliao Basin Water Environment, Ministry of Education, Jilin University of Construction for this project.

Conflicts of Interest: The authors declare no conflict of interest.

References

1. Ding, Y.; Zhao, J.; Liu, J.-W.; Zhou, J.; Cheng, L.; Zhao, J.; Shao, Z.; Iris, Ç.; Pan, B.; Li, X.; et al. A review of China's municipal solid waste (MSW) and comparison with international regions: Management and technologies in treatment and resource utilization. *J. Clean. Prod.* **2021**, *293*, 126144. [[CrossRef](#)]
2. Yu, D.; Pei, Y.; Ji, Z.; He, X.; Yao, Z. A review on the landfill leachate treatment technologies and application prospects of three-dimensional electrode technology. *Chemosphere* **2022**, *291*, 132895. [[CrossRef](#)] [[PubMed](#)]
3. Bandala, E.R.; Liu, A.; Wijesiri, B.; Zeidman, A.B.; Goonetilleke, A. Emerging materials and technologies for landfill leachate treatment: A critical review. *Environ. Pollut.* **2021**, *291*, 118133. [[CrossRef](#)] [[PubMed](#)]
4. Yuan, Y.; Liu, J.; Gao, B.; Sillanpää, M. Landfill leachate treatment in-depth by bio-chemical strategy: Microbial activation and catalytic ozonation mechanism. *Chem. Eng. J.* **2022**, *444*, 136464. [[CrossRef](#)]
5. Li, S.; Yang, Y.; Zheng, H.; Zheng, Y.; Jing, T.; Ma, J.; Nan, J.; Leong, Y.K.; Chang, J.-S. Advanced oxidation process based on hydroxyl and sulfate radicals to degrade refractory organic pollutants in landfill leachate. *Chemosphere* **2022**, *297*, 134214. [[CrossRef](#)]
6. Yan, Z.; Jiang, Y.; Chen, X.; Lu, Z.; Wei, Z.; Fan, G.; Liang, H.; Qu, F. Evaluation of applying membrane distillation for landfill leachate treatment. *Desalination* **2021**, *520*, 115358. [[CrossRef](#)]
7. Deng, Y.; Ezyske, C.M. Sulfate radical-advanced oxidation process (SR-AOP) for simultaneous removal of refractory organic contaminants and ammonia in landfill leachate. *Water Res.* **2011**, *45*, 6189–6194. [[CrossRef](#)]
8. Hassan, M.; Wang, X.; Wang, F.; Wu, D.; Hussain, A.; Xie, B. Coupling ARB-based biological and photochemical (UV/TiO₂ and UV/S₂O₈²⁻) techniques to deal with sanitary landfill leachate. *Waste Manag.* **2017**, *63*, 292–298. [[CrossRef](#)]
9. Zhang, M.; Chen, X.; Zhou, H.; Muruganathan, M.; Zhang, Y. Degradation of p-nitrophenol by heat and metal ions co-activated persulfate. *Chem. Eng. J.* **2015**, *264*, 39–47. [[CrossRef](#)]
10. Rodrigues, C.S.D.; Madeira, L.M. p-Nitrophenol degradation by activated persulfate. *Environ. Technol. Innov.* **2021**, *21*, 101265. [[CrossRef](#)]
11. Guo, R.; Chen, Y.; Liu, B.; Han, Y.; Gou, J.; Cheng, X. Catalytic degradation of lomefloxacin by photo-assisted persulfate activation on natural hematite: Performance and mechanism. *Chin. Chem. Lett.* **2022**, *33*, 3809–3817. [[CrossRef](#)]
12. Kim, C.; Ahn, J.Y.; Kim, T.Y.; Shin, W.S.; Hwang, I. Activation of Persulfate by Nanosized Zero-Valent Iron (NZVI): Mechanisms and Transformation Products of NZVI. *Environ. Sci. Technol.* **2018**, *52*, 3625–3633. [[CrossRef](#)] [[PubMed](#)]
13. Choekjaroenrat, C.; Sakulthaew, C.; Angkaew, A.; Satapanajaru, T.; Poapolathep, A.; Chirasatienpon, T. Remediating sulfadimethoxine-contaminated aquaculture wastewater using ZVI-activated persulfate in a flow-through system. *Aquac. Eng.* **2019**, *84*, 99–105. [[CrossRef](#)]
14. Singh, N.; Qutub, S.; Khashab, N.M. Biocompatibility and biodegradability of metal organic frameworks for biomedical applications. *J. Mater. Chem. B* **2021**, *9*, 5925–5934. [[CrossRef](#)] [[PubMed](#)]

15. Sabatino, R.; Furia, F.; Eckert, E.M.; Minella, M.; Corno, G.; Di Cesare, A.; Vione, D. The ZVI-Fenton process affects the total load of human pathogenic bacteria in wastewater samples. *J. Water Process Eng.* **2022**, *47*, 102668. [[CrossRef](#)]
16. Zhang, H.; Zhang, D.; Zhou, J. Removal of COD from landfill leachate by electro-Fenton method. *J. Hazard. Mater.* **2006**, *135*, 106–111. [[CrossRef](#)]
17. Luu, T.L. Post treatment of ICEAS-biologically landfill leachate using electrochemical oxidation with Ti/BDD and Ti/RuO₂ anodes. *Environ. Technol. Innov.* **2020**, *20*, 101099. [[CrossRef](#)]
18. Oturan, N.; van Hullebusch, E.D.; Zhang, H.; Mazéas, L.; Budzinski, H.; Le Ménach, K.; Oturan, M.A. Occurrence and Removal of Organic Micropollutants in Landfill Leachates Treated by Electrochemical Advanced Oxidation Processes. *Environ. Sci. Technol.* **2015**, *49*, 12187–12196. [[CrossRef](#)]
19. Zhou, T.; Du, J.; Wang, Z.; Xiao, G.; Luo, L.; Faheem, M.; Ling, H.; Bao, J. Degradation of sulfamethoxazole by MnO₂/heat-activated persulfate: Kinetics, synergistic effect and reaction mechanism. *Chem. Eng. J. Adv.* **2022**, *9*, 100200. [[CrossRef](#)]
20. Salehi, H.; Ebrahimi, A.A.; Ehrampoush, M.H.; Salmani, M.H.; Fard, R.F.; Jalili, M.; Gholizadeh, A. Integration of photo-oxidation based on UV/Persulfate and adsorption processes for arsenic removal from aqueous solutions. *Groundw. Sustain. Dev.* **2020**, *10*, 100338. [[CrossRef](#)]
21. Dhaka, S.; Kumar, R.; Khan, M.A.; Paeng, K.-J.; Kurade, M.B.; Kim, S.-J.; Jeon, B.-H. Aqueous phase degradation of methyl paraben using UV-activated persulfate method. *Chem. Eng. J.* **2017**, *321*, 11–19. [[CrossRef](#)]
22. Hussain, I.; Li, M.; Zhang, Y.; Huang, S.; Hayat, W.; Li, Y.; Du, X.; Liu, G. Efficient oxidation of arsenic in aqueous solution using zero valent iron- activated persulfate process. *J. Environ. Chem. Eng.* **2017**, *5*, 3983–3990. [[CrossRef](#)]
23. Wang, J.; Wang, S. Activation of persulfate (PS) and peroxymonosulfate (PMS) and application for the degradation of emerging contaminants. *Chem. Eng. J.* **2018**, *334*, 1502–1517. [[CrossRef](#)]
24. Chen, G.; Wu, G.; Li, N.; Lu, X.; Zhao, J.; He, M.; Yan, B.; Zhang, H.; Duan, X.; Wang, S. Landfill leachate treatment by persulfate related advanced oxidation technologies. *J. Hazard. Mater.* **2021**, *418*, 126355. [[CrossRef](#)]
25. Huang, L.; Li, Z.; Wang, G.; Zhao, W.; Xu, Y.; Wang, D. Experimental study on advanced treatment of landfill leachate by ultraviolet catalytic persulfate. *Environ. Technol. Innov.* **2021**, *23*, 101794. [[CrossRef](#)]
26. Kim, C.; Ahn, J.-Y.; Kim, T.Y.; Hwang, I. Mechanisms of electro-assisted persulfate/nano-Fe₀ oxidation process: Roles of redox mediation by dissolved Fe. *J. Hazard. Mater.* **2020**, *388*, 121739. [[CrossRef](#)]
27. Ghahrchi, M.; Rezaee, A. Electro-catalytic ozonation for improving the biodegradability of mature landfill leachate. *J. Environ. Manag.* **2019**, *254*, 109811. [[CrossRef](#)]
28. Mirehbar, S.; Fernández-Velayos, S.; Mazario, E.; Menéndez, N.; Herrasti, P.; Recio, F.J.; Sirés, I. Evidence of cathodic peroxydisulfate activation via electrochemical reduction at Fe(II) sites of magnetite-decorated porous carbon: Application to dye degradation in water. *J. Electroanal. Chem.* **2021**, *902*, 115807. [[CrossRef](#)]
29. Zou, L.; Wang, Y.; Huang, C.; Li, B.; Lyu, J.; Wang, S.; Lu, H.; Li, J. Meta-cresol degradation by persulfate through UV/O₃ synergistic activation: Contribution of free radicals and degradation pathway. *Sci. Total Environ.* **2021**, *754*, 142219. [[CrossRef](#)]
30. Chin, Y.P.; Aiken, G.R.; Danielsen, K.M. Binding of pyrene to aquatic and commercial humic substances: The role of molecular weight and aromaticity. *Environ. Sci. Technol.* **1997**, *31*, 1630–1635. [[CrossRef](#)]
31. Nishijima, W.; Speitel, G.E. Fate of biodegradable dissolved organic carbon produced by ozonation on biological activated carbon. *Chemosphere* **2004**, *56*, 113–119. [[CrossRef](#)] [[PubMed](#)]
32. Gu, Z.; Chen, W.; Li, Q.; Zhang, A. Treatment of semi-aerobic aged-refuse biofilter effluent from treating landfill leachate with the Fenton method. *Process Saf. Environ. Prot.* **2020**, *133*, 32–40. [[CrossRef](#)]
33. Xu, J.; Long, Y.; Shen, D.; Feng, H.; Chen, T. Optimization of Fenton treatment process for degradation of refractory organics in pre-coagulated leachate membrane concentrates. *J. Hazard. Mater.* **2017**, *323*, 674–680. [[CrossRef](#)] [[PubMed](#)]
34. Carstea, E.M.; Baker, A.; Bieroza, M.; Reynolds, D.M.; Bridgeman, J. Characterisation of dissolved organic matter fluorescence properties by PARAFAC analysis and thermal quenching. *Water Res.* **2014**, *61*, 152–161. [[CrossRef](#)]
35. Moradian, F.; Ramavandi, B.; Jaafarzadeh, N.; Kouhgard, E. Effective treatment of high-salinity landfill leachate using ultraviolet/ultrasonication/ peroxymonosulfate system. *Waste Manag.* **2020**, *118*, 591–599. [[CrossRef](#)]
36. Li, J.; Wan, Y.; Li, Y.; Yao, G.; Lai, B. Surface Fe(III)/Fe(II) cycle promoted the degradation of atrazine by peroxymonosulfate activation in the presence of hydroxylamine. *Appl. Catal. B Environ.* **2019**, *256*, 117782. [[CrossRef](#)]
37. Huang, C.; Wang, Y.; Gong, M.; Wang, W.; Mu, Y.; Hu, Z.-H. α -MnO₂/Palygorskite composite as an effective catalyst for heterogeneous activation of peroxymonosulfate (PMS) for the degradation of Rhodamine B. *Sep. Purif. Technol.* **2020**, *230*, 115877. [[CrossRef](#)]
38. Milh, H.; Schoenaers, B.; Stesmans, A.; Cabooter, D.; Dewil, R. Degradation of sulfamethoxazole by heat-activated persulfate oxidation: Elucidation of the degradation mechanism and influence of process parameters. *Chem. Eng. J.* **2020**, *379*, 122234. [[CrossRef](#)]
39. Zhang, B.-T.; Zhang, Y.; Teng, Y.; Fan, M. Sulfate Radical and Its Application in Decontamination Technologies. *Crit. Rev. Environ. Sci. Technol.* **2015**, *45*, 1756–1800. [[CrossRef](#)]
40. Wang, Z.; Li, J.; Tan, W.; Wu, X.; Lin, H.; Zhang, H. Removal of COD from landfill leachate by advanced Fenton process combined with electrolysis. *Sep. Purif. Technol.* **2019**, *208*, 3–11. [[CrossRef](#)]
41. Tripathy, B.K.; Kumar, M. Sequential coagulation/flocculation and microwave-persulfate processes for landfill leachate treatment: Assessment of bio-toxicity, effect of pretreatment and cost-analysis. *Waste Manag.* **2019**, *85*, 18–29. [[CrossRef](#)] [[PubMed](#)]

42. Li, M.; Qin, X.; Gao, M.; Li, T.; Lv, Y. Graphitic carbon nitride and carbon nanotubes modified active carbon fiber cathode with enhanced H₂O₂ production and recycle of Fe³⁺/Fe²⁺ for electro-Fenton treatment of landfill leachate concentrate. *Environ. Sci. Nano* **2022**, *9*, 632–652. [[CrossRef](#)]
43. Sun, W.-Q.; Hu, J.-B.; Jiang, Y.-J.; Xu, N.; Wang, L.-Y.; Li, J.-H.; Hu, Y.-Q.; Duttwyler, S.; Zhang, Y.-B. Flexible molecular sieving of C₂H₂ from CO₂ by a new cost-effective metal organic framework with intrinsic hydrogen bonds. *Chem. Eng. J.* **2022**, *439*, 135745. [[CrossRef](#)]
44. Wang, X.; Li, H.; Quan, K.; Zhao, L.; Li, Z.; Qiu, H. Anhydride-linked β-cyclodextrin-bonded silica stationary phases with enhanced chiral separation ability in liquid chromatography. *J. Chromatogr. A* **2021**, *1651*, 462338. [[CrossRef](#)] [[PubMed](#)]
45. Vlyssides, A.G.; Karlis, P.K.; Mahnken, G. Influence of various parameters on the electrochemical treatment of landfill leachates. *J. Appl. Electrochem.* **2003**, *33*, 155–159. [[CrossRef](#)]
46. Panizza, M.; Delucchi, M.; Sirés, I. Electrochemical process for the treatment of landfill leachate. *J. Appl. Electrochem.* **2010**, *40*, 1721–1727. [[CrossRef](#)]
47. Yazici Guvenc, S.; Dincer, K.; Varank, G. Performance of electrocoagulation and electro-Fenton processes for treatment of nanofiltration concentrate of biologically stabilized landfill leachate. *J. Water Process Eng.* **2019**, *31*, 100863. [[CrossRef](#)]